Title
Distribution and function of monoacylglycerol lipase in the gastrointestinal tract

Journal
AJP Gastrointestinal and Liver Physiology, 295(6)

ISSN
0193-1857

Authors
Duncan, Marnie
Thomas, Adam D
Cluny, Nina L
et al.

Publication Date
2008-12-01

DOI
10.1152/ajpgi.90500.2008

Am J Physiol Gastrointest Liver Physiol 295: G1255–G1265, 2008.
First published October 23, 2008; doi:10.1152/ajpgi.90500.2008.

Distribution and function of monoacylglycerol lipase in the gastrointestinal tract

Marnie Duncan,[1] Adam D. Thomas,[1] Nina L. Cluny,[1] Annie Patel,[2] Kamala D. Patel,[1] Beat Lutz,[3] Daniele Piomelli,[4] Stephen P. H. Alexander,[2] and Keith A. Sharkey[1]

[1]*Hotchkiss Brain Institute and Snyder Institute of Infection, Immunity and Inflammation, Department of Physiology and Biophysics, University of Calgary, Calgary, Alberta, Canada;* [2]*School of Biomedical Sciences and Institute of Neuroscience, University of Nottingham Medical School, Nottingham, United Kingdom;* [3]*Department of Physiological Chemistry, Johannes Gutenberg University Mainz, Mainz, Germany; and* [4]*Department of Pharmacology, University of California, Irvine, California*

Submitted 18 August 2008; accepted in final form 17 October 2008

Duncan M, Thomas AD, Cluny NL, Patel A, Patel KD, Lutz B, Piomelli D, Alexander SP, Sharkey KA. Distribution and function of monoacylglycerol lipase in the gastrointestinal tract. *Am J Physiol Gastrointest Liver Physiol* 295: G1255–G1265, 2008. First published October 23, 2008; doi:10.1152/ajpgi.90500.2008.—The endogenous cannabinoid system plays an important role in the regulation of gastrointestinal function in health and disease. Endocannabinoid levels are regulated by catabolic enzymes. Here, we describe the presence and localization of monoacylglycerol lipase (MGL), the major enzyme responsible for the degradation of 2-arachidonoylglycerol. We used molecular, biochemical, immunohistochemical, and functional assays to characterize the distribution and activity of MGL. MGL mRNA was present in rat ileum throughout the wall of the gut. MGL protein was distributed in the muscle and mucosal layers of the ileum and in the duodenum, proximal colon, and distal colon. We observed MGL expression in nerve cell bodies and nerve fibers of the enteric nervous system. There was extensive colocalization of MGL with PGP 9.5 and calretinin-immunoreactive neurons, but not with nitric oxide synthase. MGL was also present in the epithelium and was highly expressed in the small intestine. Enzyme activity levels were highest in the duodenum and decreased along the gut with lowest levels in the distal colon. We observed both soluble and membrane-associated enzyme activities. The MGL inhibitor URB602 significantly inhibited whole gut transit in mice, an action that was abolished in cannabinoid 1 receptor-deficient mice. In conclusion, MGL is localized in the enteric nervous system where endocannabinoids regulate intestinal motility. MGL is highly expressed in the epithelium, where this enzyme may have digestive or other functions yet to be determined.

endocannabinoids; enteric nervous system; URB602; 2-arachidonoyl glycerol

CANNABINOID (CB) receptors (termed CB_1 and CB_2), the endogenous ligands for these receptors (endocannabinoids), and their biosynthetic and catabolic enzymes form the endocannabinoid system (11, 12). This novel regulatory system has important roles in physiology and has been linked to a number of pathophysiological conditions, notably disorders of energy metabolism (31). There is increasing evidence for significant roles of the endocannabinoid system in the control of gastrointestinal and liver (patho)physiology (15, 22, 37, 44, 45, 47).

CB_1 receptors are predominantly expressed in the enteric nervous system (ENS), where they are primarily localized to prejunctional nerve terminals and regulate transmitter release (15). We recently described the localization of CB_2 receptors in the ENS (16). These receptors appear to be active under pathophysiological conditions and serve to limit the extent of enhanced motility seen under these circumstances (30). The natural endogenous ligands for the CB receptors, anandamide and 2-arachidonoylglycerol (2-AG), have affinity at both CB_1 and CB_2 receptors (10, 21, 32). Unlike classical transmitters, endocannabinoids are synthesized and released "on demand." Recently, their biosynthetic and inactivation pathways have been identified. Anandamide is an *N*-acylethanolamine formed from the cleavage of *N*-arachidonoyl phosphatidylethanolamine catalyzed by a unique phospholipase D (1). The biosynthesis of 2-AG comprises the sequential action of phospholipase C and diacylglycerol lipase (DGL) on membrane phospholipid (1, 42). Anandamide and 2-AG are present within the gastrointestinal (GI) tract at levels able to activate CB receptors. Anandamide is present in ileal and colonic tissues at levels of 0.27 and 0.036 nmol/g, whereas 2-AG levels are 44.1 and 18.7 nmol/g, respectively (38). Such regional differences of endocannabinoids along the GI tract may reflect functional differences in their actions in the ileum and colon.

Inactivation pathways for endocannabinoids are thought to involve a putative endocannabinoid membrane transporter (11, 12, 33). Once taken up into the cell they are degraded by the enzymes fatty acid amide hydrolase (FAAH; also known as anandamide amidohydrolase) and monoacylglycerol lipase (MGL; also known as monoglyceride lipase) (8, 9, 13, 14, 17). FAAH has been shown to catalyze the hydrolysis of both anandamide and 2-AG (8, 9, 17). FAAH mRNA and protein expression is present in the GI tract (4) and inhibition significantly attenuates intestinal motility in mice, indicating that enhanced local endocannabinoid levels are functionally significant (23). Genetic ablation of FAAH in mice results in a 2.8-fold increase of ileal anandamide content with respect to wild-type controls (4), and these mice are significantly protected against inflammation in the 2,4-dinitrobenzene sulfonic acid model of experimental colitis (29).

The second enzyme involved in endocannabinoid inactivation, MGL, is a serine hydrolase that converts 2-AG to fatty acids and glycerol (13). MGL mRNA and protein have been localized to nerve fibers and soma in areas of the brain that

Address for reprint requests and other correspondence: K. Sharkey, Dept. of Physiology and Biophysics, Univ. of Calgary, 3330 Hospital Dr. NW, Calgary, Alberta, Canada T2N 4N1 (e-mail: ksharkey@ucalgary.ca).

The costs of publication of this article were defrayed in part by the payment of page charges. The article must therefore be hereby marked "*advertisement*" in accordance with 18 U.S.C. Section 1734 solely to indicate this fact.

express high levels of CB_1 receptors (13). URB602 is a rapidly acting, noncompetitive inhibitor of MGL (25) that increases 2-AG levels in hippocampal slice cultures (25, 27) and enhances stress-induced analgesia by raising local 2-AG levels when administered into the periaqueductal gray matter (20). However, more recent papers have described antinociceptive actions of URB602 when administered intraperitoneally and subcutaneously in the carrageenan and formalin inflammatory pain models, respectively (6, 18).

Although a physiological role of FAAH has been described in the GI tract (4, 38), the distribution and function of MGL within the GI tract is unknown. The purpose of this study was to examine the distribution and function of MGL in the rodent GI tract to provide a better understanding of the endocannabinoid system within the gut.

MATERIALS AND METHODS

Animals. Male Sprague-Dawley rats (250–350 g; Charles River Laboratories, Montreal, QC, Canada), male C57BL/6 mice (5–6 wk; 20–26 g) or female $CB_1^{-/-}$ mice (8 wk; 18–22 g) on a C57BL/6 background were used for our studies. The C57BL/6 mice were obtained from Charles River (Montreal, QC, Canada). Two breeding pairs of heterozygous $CB_1^{+/-C57BL/6N}$ (28) mice were obtained from Dr. Beat Lutz (Johannes Gutenberg University Mainz, Mainz, Germany) and bred in our facility to obtain $CB_1^{-/-C57BL/6N}$ mice. Animals used in these studies were backcrossed from both heterozygous and homozygous breeding pairs to C57BL/6N for six generations and were maintained under the same conditions as the wild-type mice. All $CB_1^{-/-}$ mice were genotyped by established protocols and were confirmed as homozygous gene-deficient animals ($CB_1^{-/-C57BL/6N}$) prior to inclusion in the study. Animals were housed in a temperature-controlled room, maintained on a normal 12:12-h light-dark cycle, in plastic sawdust floor cages with free access to Purina Laboratory chow and tap water. These studies were approved by the University of Calgary Animal Care Committee, and all protocols were carried out in accordance with the guidelines of the Canadian Council on Animal Care.

Tissue preparation. Rats were deeply anesthetized with an intraperitoneal injection of pentobarbital sodium (65 mg/kg). Tissues used for RT-PCR, Western blotting, and enzyme assays were taken from animals perfused intracardially with 1 l/kg phosphate-buffered saline (PBS) to remove the blood and stored at −80°C until use. Tissue for immunohistochemistry ($n = 5$) were removed, washed, pinned flat onto a Sylgard-coated plate, and immersed in Zamboni's fixative (2% paraformaldehyde and 0.2% picric acid; pH 7.4) overnight at 4°C. Tissues used for sectioning were stapled flat on a cardboard mount, fixed in Zamboni's fixative, and then cryoprotected in sucrose (20% in PBS) in preparation for sectioning.

RT-PCR. Total RNA was isolated by use of TRIzol reagent (Invitrogen, Carlsbad, CA). RNA was reverse transcribed into cDNA by using Superscript II reverse transcriptase (Invitrogen) according to manufacturer's instructions. PCR for MGL and β-actin was performed with 10% of the RT reaction as template cDNA by using Qiagen Master Mix (Qiagen, Gaithersburg, MD) according to manufacturer's recommendations. The primers used were MGL forward: 5′-TAGCAGCTGCAGAGAGACCA-3′, MGL reverse: 5′-GATGAGTGGGTCGGAGTTGT-3′, β-actin forward: 5′-GCTGCTCACCGAGGC-3′, and β-actin reverse: 5′-CTCGGTCAGGATCTTCAT-3′. Target cDNAs were amplified by 25 cycles of 1 min at 94°C, 1 min at 65°C, and 1 min at 72°C. The PCR product was run through an agarose gel and bands were visualized with ethidium bromide.

Western blotting. For the first experiment, full-thickness ileal segments, muscle and submucosal layers (containing the ENS), and mucosa (removed by scraping the opened intestine with a microscope slide, $n = 6$) were collected. For the second experiment, full-thickness tissues were collected from duodenum, ileum, and proximal and distal colon ($n = 5$). Samples were immediately suspended in enzyme inhibitors (11697498001; Roche Diagnostics, Indianapolis, IN) and homogenized, and protein concentrations were determined. Proteins were separated with SDS-PAGE (10%), then transferred onto a nitrocellulose membrane, as previously described (34). Membranes were then incubated in blocking solution composed of 5% fat-free milk and Tris-buffered saline for 1 h at room temperature followed by overnight incubation with an immunopurified polyclonal antibody directed against the NH_2 terminal of MGL (peptide sequence SSPRRTPQNVPYQDL; Dr. Daniele Piomelli, University of California Irvine, Irvine, CA) (13, 14) at 4°C. Membranes were washed with Tris-buffered saline with Triton X-100 and incubated in a horseradish peroxidase-conjugated goat anti-rabbit antibody (1:4,000; Santa Cruz Biotechnology, sc-2004, Santa Cruz, CA) for 1 h at room temperature. Protein bands were visualized by use of a chemiluminescent substrate (ECL kit; Amersham, Little Chalfont, Bucks, UK) and X-Omat film (Eastman Kodak, Rochester, NY). The same membranes were stripped and reblotted with rabbit anti-actin (Sigma-Aldrich, A2066, St. Louis, MO) and a secondary antibody. Proteins were semiquantitatively analyzed by densitometric measurement of the bands.

Immunohistochemistry. Whole-mount preparations of longitudinal muscle-myenteric plexus (MP) and submucosal plexus (SMP) were prepared as previously described (41). Briefly, the mucosa was removed, the submucosal layer was then carefully separated from the layers beneath, and then the circular muscle layer was separated from the longitudinal muscle layer, to which the MP remained adhered. Single- and double-labeling immunohistochemistry were used in the following regions of the GI tract: duodenum, ileum, proximal colon, and distal colon. In further experiments, double labeling for specific neuronal markers was used to determine whether MGL was associated with specific neuronal subpopulations. Double labeling was carried out in a sequential manner. Briefly, tissues were first incubated in either mouse anti-PGP 9.5 (1:500; 13C4, Ultraclone, Cedarlane Laboratories, Burlington, ON, Canada), goat anti-calretinin (1:500; CG1, Swant, Bellizona, Switzerland) or mouse antineuronal nitric oxide synthase (NOS; 1:250, N-2280, Sigma-Aldrich) for 48 h at 4°C. Tissues were then washed in PBS, three times for 30 min, and then incubated in the secondary antibodies goat anti-mouse FITC (1:50; 115-095-003, Jackson, West Grove, PA) or donkey anti-goat FITC (1:50; 705-095-147, Jackson) for 2 h at room temperature. Tissues were then washed in PBS and subsequently incubated with rabbit anti-MGL (Dr. Daniele Piomelli, University of California Irvine) (13; 14) and donkey anti-rabbit CY3 (1:100; 711-165-152, Jackson). Tissues were then mounted on slides with a bicarbonate-buffered glycerol (pH 8.6) and visualized with either a Zeiss Axioplan fluorescence microscope or an Olympus Fluoview FV300 confocal microscope. Corel Photopaint was used to adjust all images for brightness, contrast, and intensity. To quantify MGL expressing neurons in the ENS, a ratio of MGL-positive neurons to PGP 9.5/calretinin-positive neurons was determined. MGL or PGP 9.5/calretinin-positive cells were counted in 15 (MP) or 20 (SMP) ganglia in whole-mount preparations ($n = 3$).

Enzyme activity. Frozen tissue segments were thawed and homogenized in 10 volumes of TE buffer (50 mM Tris, 1 mM EDTA, pH 7.4) by using a Polytron homogenizer. Following centrifugation at 30,000 *g* for 30 min, the supernatant layer was collected and the pellet was homogenized once more in 10 volumes of TE buffer. Following centrifugation as before, the supernatant layers were combined and stored at −80°C. The pellet was resuspended in three volumes of 50 mM Tris buffer, pH 7.4, and stored at −80°C. Assays of MGL activity were conducted using minor modifications of methods described by Vandevoorde et al. (46). In brief, thawed samples were diluted in TE buffer to a suitable protein concentration (~1:100 wet wt for particulate preparations and ~1:1,000 for soluble fractions) and preincubated with inhibitor at 37°C for 10 min, before addition of 2-oleoylglycerol (2-OG, 100 μM, Sigma-Aldrich; containing 1–2 kBq

2-oleoyl-[^{3}H]-glycerol, American Radiolabeled Chemicals). After incubation at 37°C for 15 min, the reaction was terminated by the addition of two volumes of chloroform-methanol (1:1) and mixing. Chloroform (1 volume) was added to separate the phases, before removal of an aliquot of the supernatant layer containing liberated [^{3}H]glycerol for liquid scintillation counting.

Upper GI transit studies. After an overnight fasting period (water ad libitum), a marker was administered orally to assess upper GI transit, as described in detail by others (39, 40). At 30 min after intraperitoneal (ip) administration of URB602 (20 or 40 mg/kg) or vehicle [10% DMSO/Tween 80 in saline (6)], an oral gavage of 200 μl of an Evans blue marker (5% Evans blue, 5% gum arabic) was administered. After 15 min animals were killed by cervical dislocation and the intestine from the region of the pyloric sphincter to the ileocecal junction was immediately removed. The distance traveled by the marker was measured in centimeters and expressed as a percentage of the total length of the small intestine.

Colonic propulsion. Distal colonic propulsion was measured according to the method of Broccardo et al. (3). Briefly, 30, 150, and 270 min after ip administration of URB602 (20 or 40 mg/kg) or vehicle [10% DMSO/Tween 80 in saline (6)], a 2.5-mm spherical plastic bead was inserted 3 cm intrarectally to mice lightly anesthetized with isoflurane. This bead size was chosen after preliminary experiments and was based on the size of an average fecal pellet. The time to expulsion of the plastic bead was determined for each animal in seconds and data were expressed as the mean of the three values. A higher mean expulsion time value is an index of inhibition of colonic propulsion. It should be noted that this assay reflects colonic propulsion as well as sensory threshold of the pellet in the colon, hence our use of "physiological" pellets.

Whole gut transit studies. After a 1-h acclimatization to individual plastic cages, without a sawdust floor or bedding, mice were administered an intraperitoneal (ip) injection of URB602 (20 or 40 mg/kg) or vehicle [10% DMSO/Tween 80 in saline (6)] 30 min before receiving an oral gavage (via a 3-cm, 20-G gavaging needle) of 200 μl of an Evans blue marker. Mice were returned to their individual cages (ad libitum access to food and water) and the latency to the detection of Evans blue in the droppings was recorded. In further experiments $CB_1^{-/-}$ mice were administered an ip injection of URB602 (40 mg/kg) or vehicle and whole gut transit time was measured as outlined above.

Statistical analysis. Data are expressed as means ± SE and analyzed with Student's *t*-tests or by a one-way analysis of variance with Bonferroni-corrected *t*-tests. $P < 0.05$ was considered significant.

RESULTS

MGL mRNA is present in the rat ileum. MGL mRNA was present in samples of full-wall-thickness ileum, as well as in the muscle and submucosal layers that contain the ENS and the mucosa (Fig. 1*A*). No band was detected in the absence of the template. RNA from the samples were reverse transcribed or mock-treated prior to PCR. We observed no bands in the RNA sample that was mock treated, indicating that amplification was not due to genomic DNA contamination of the RNA sample (data not shown).

MGL protein is expressed throughout the rat GI tract. Western blot analyses confirmed the presence of MGL protein in homogenates of rat ileal tissue (Fig. 1*B*). MGL was detected in full-wall-thickness samples of ileum and was also present in the muscle and submucosal layers and the mucosa. The bands were ~33 kDa, which is an appropriate molecular mass on the basis of previously published work (14, 24). Preabsorption of this antibody with the immunizing peptide has previously been shown to abolish detection of bands (14). Semiquantitative densitometric measurement, expressed as a ratio of actin content in each sample, indicated that the muscle and submucosal layer containing the enteric plexuses had higher levels of MGL expression compared with the mucosa (Fig. 1*C*). MGL is expressed along the length of the GI tract in the full-wall-thickness samples of duodenum, ileum, proximal colon, and distal colon (Fig. 1*B*). The lowest levels were found in the duodenum, whereas no significant differences were found between the levels in ileum, proximal colon, and distal colon (Fig. 1*D*). In the proximal colon, we observed a fairly promi-

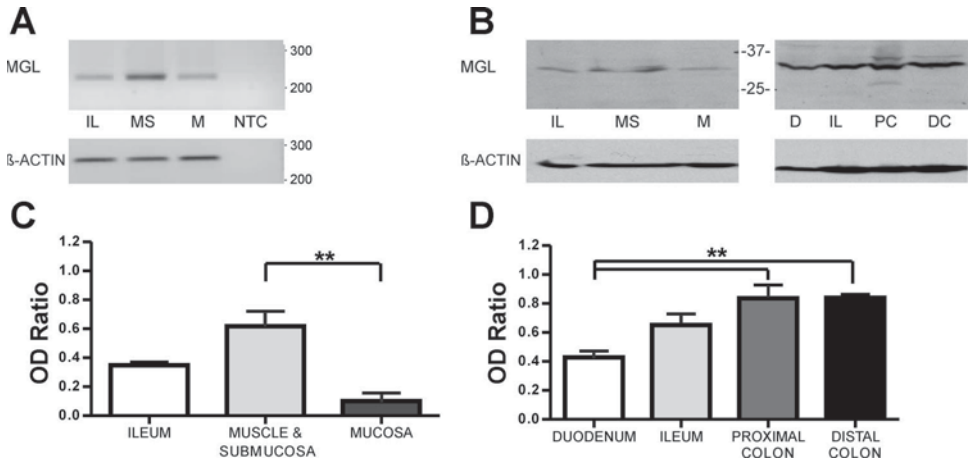

Fig. 1. Monoacylglycerol lipase (MGL) mRNA and protein are expressed throughout the gastrointestinal (GI) tract. *A*: RNA was isolated from full-wall-thickness ileum (IL), muscle layer containing myenteric plexus and submucosa (MS), and mucosa (M) of rats. PCR was performed using primers for MGL or β-actin and the expected amplicons were 212 and 277 bp, respectively. No band was detected in the no-template control (NTC). *B*: protein homogenates were isolated from the full-wall-thickness ileum, muscle and submucosal layers, and mucosa of rats. Samples of full-wall-thickness duodenum, ileum, proximal colon, and distal colon were also analyzed. Western blotting was performed with an antibody directed against the NH_2 terminus of MGL and a band was observed at ~33 kDa, with an additional band observed in the proximal colon sample. *C*: semiquantitative densitometric measurement of MGL expression, expressed as a ratio of β-actin content in each sample, indicates highest expression in the muscle and submucosal layers (**$P < 0.01$ vs. mucosa). *D*: quantification of MGL levels within select regions of the GI tract indicates lowest levels in the duodenum and ileum, with higher expression in the proximal (**$P < 0.01$ vs. duodenum) and distal colon (**$P < 0.01$ vs. duodenum).

nent double band, which has also been reported in brain homogenates and may be explained by the presence of different MGL isoforms owing to different leader sequences reported in MGL cDNA (14, 24).

MGL is expressed by enteric neurons and in the epithelium of the GI tract. Cross sections of the duodenum, ileum, and proximal and distal colon showed MGL immunoreactivity to be most intense within the MP with relatively lower levels in the SMP (Fig. 2). MGL staining was also observed at the base of the crypts and within the epithelium, notably in the small intestine (Fig. 2, *left*). In whole-mount preparations, MGL immunoreactivity was present in neurons and nerve fibers within both the SMP and SMP along the rat GI tract (Figs. 3 and 4). We observed that the duodenum and ileum had more fibrous staining than the other regions of the gut (Figs. 3, *A* and *B* and 4, *A* and *B*).

PGP 9.5, a marker of neuronal populations within the ENS, was used for double staining with MGL. Cell counts were used to quantify the number of cells per ganglia that expressed MGL as a percentage of PGP 9.5-positive neurons. Most of the PGP

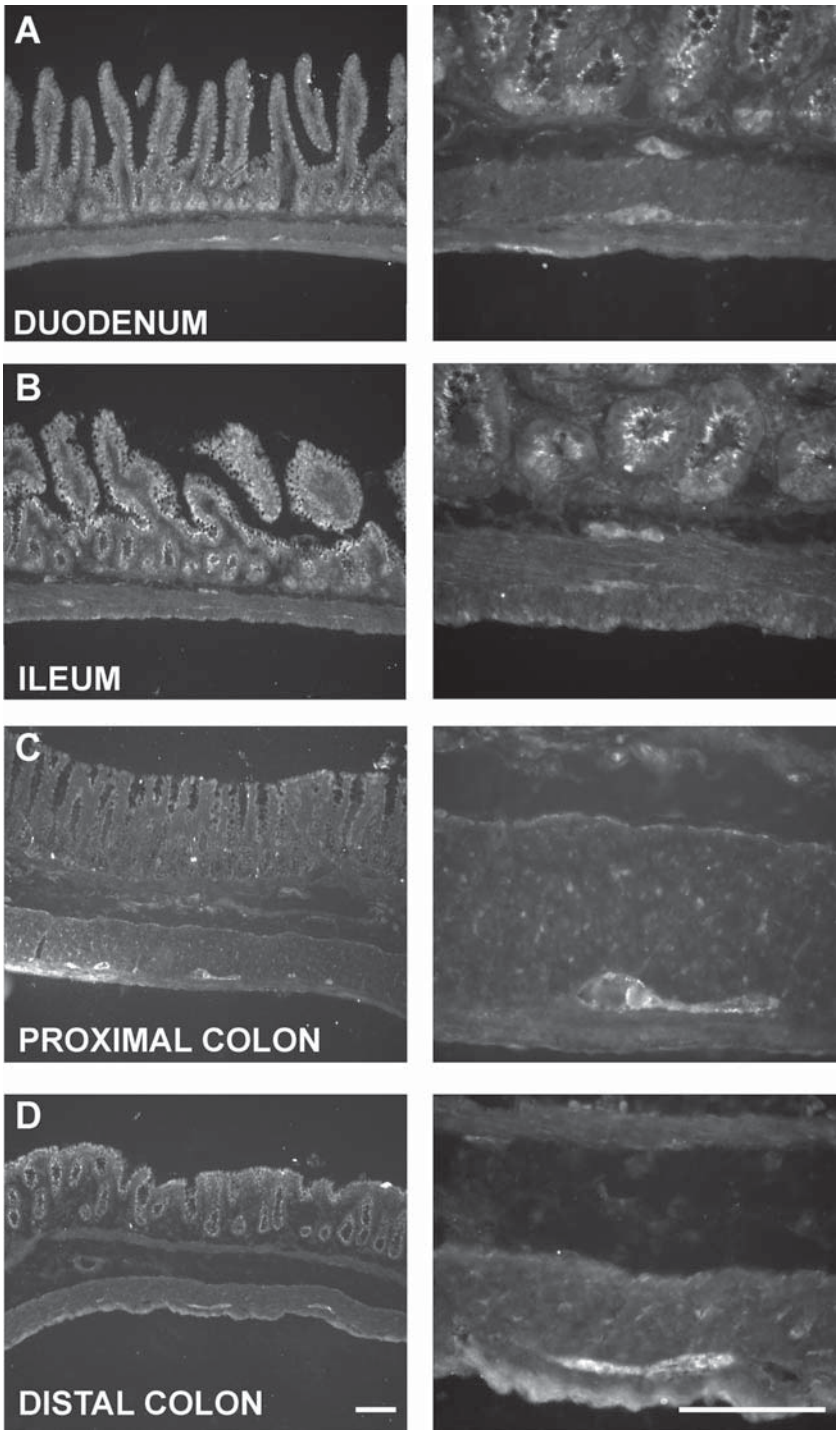

Fig. 2. Cross sections of rat duodenum (*A*), ileum (*B*), proximal colon (*C*), and distal colon (*D*). Low-power sections (*left*) and higher magnification of parts of these panels (*right*). Intense immunoreactivity was observed in the myenteric and submucosal plexus and epithelia. Scale bars: 100 μm.

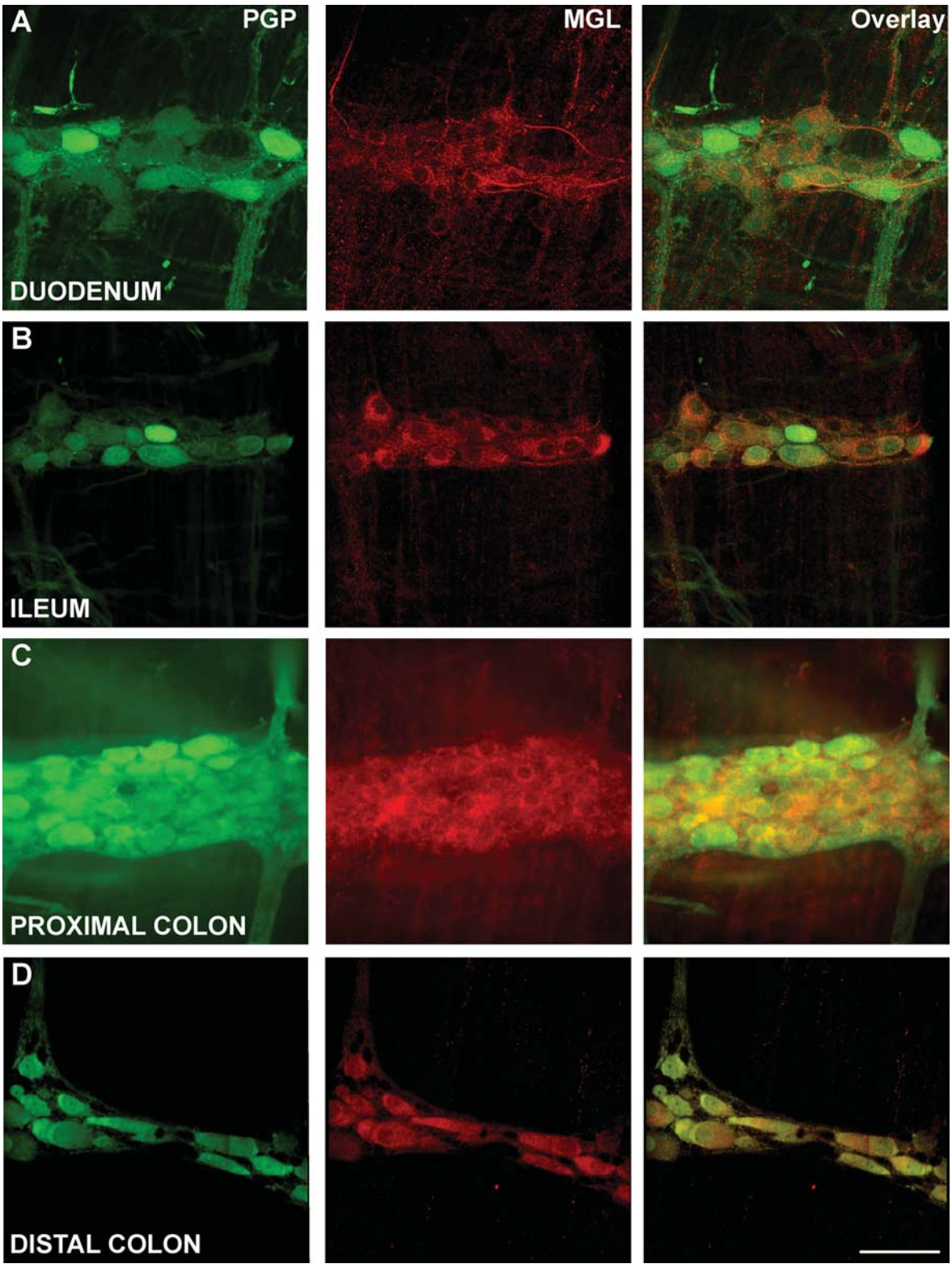

Fig. 3. Fluorescence micrographs of MGL immunoreactivity double-labeled with enteric neuronal marker PGP 9.5 (PGP) in whole-mount preparations of myenteric plexus along the rat GI tract. Single labels for PGP 9.5 (green) are in the first column, MGL immunoreactivity (red) is shown in the second column, and the overlay image is shown in the third column for duodenum (*A*), ileum (*B*), proximal colon (*C*), and distal colon (*D*). The majority of MGL-expressing enteric neurons colocalize with PGP 9.5 immunoreactivity. MGL immunoreactivity was found in the soma and processes of enteric neurons in the duodenum and ileum but tended to be found only in the soma in the colon. Scale bar: 50 μm.

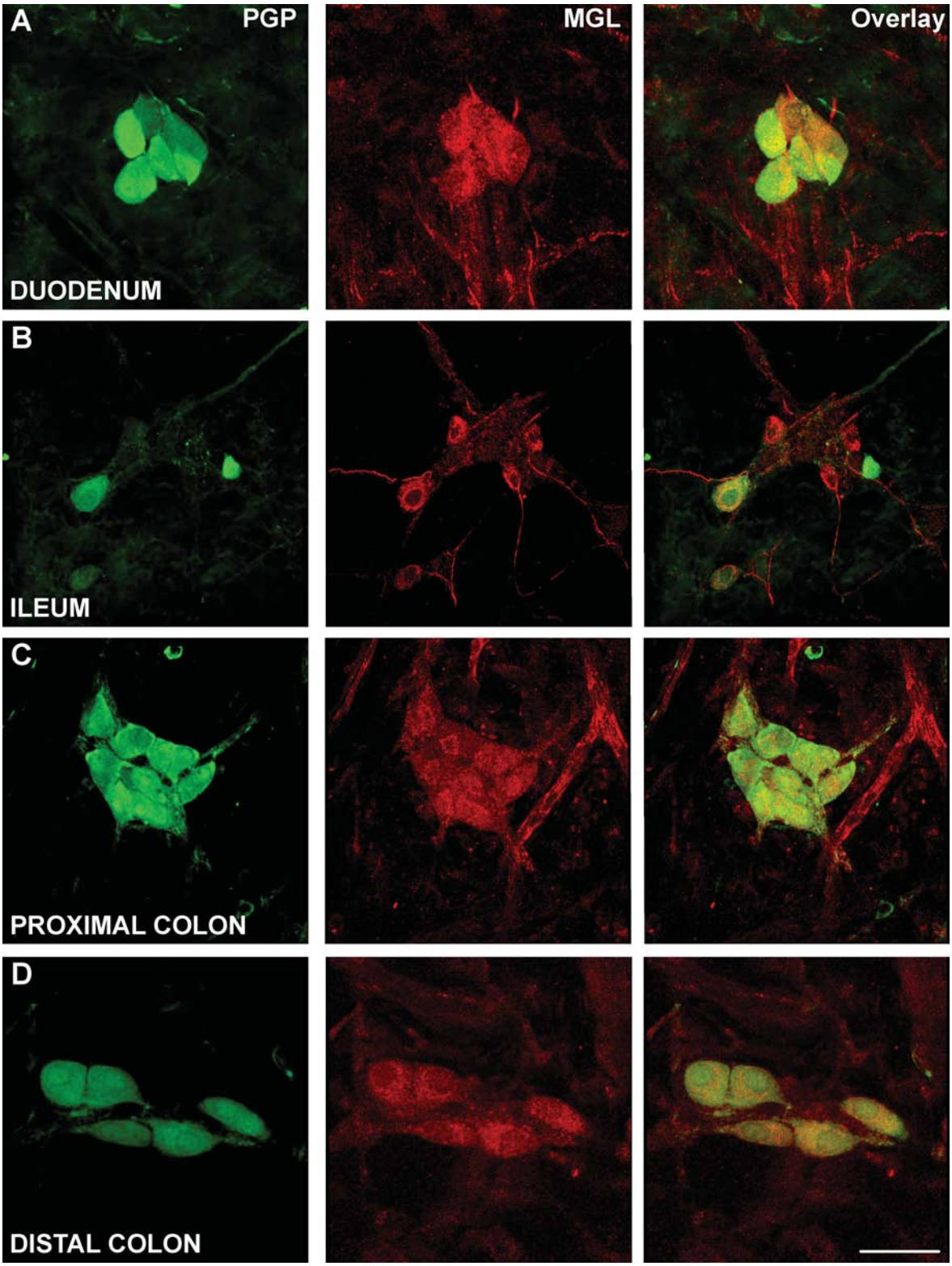

Fig. 4. Confocal fluorescence micrographs of MGL immunoreactivity double labeled with the enteric neuronal marker PGP 9.5 in whole-mount preparations of submucosal plexus along the rat gastrointestinal tract. Single labels for PGP 9.5 (green) are in the first column, MGL immunoreactivity (red) is shown in the second column, and the overlay image is shown in the third column for duodenum (*A*), ileum (*B*), proximal colon (*C*), and distal colon (*D*). The majority of MGL-expressing enteric neurons colocalize with PGP 9.5 immunoreactivity. Scale bar: 50 μm.

9.5-labeled neurons also expressed MGL: duodenum (90.2 ± 1.5%), ileum (86.5 ± 1.7%), proximal colon (82.0 ± 2.2%), and distal colon (86.7 ± 2.0%). There were no significant regional differences noted. Mean values within the SMP were as follows: duodenum (89.9 ± 1.7%), ileum (86.5 ± 1.9%), proximal colon (82.6 ± 2.1%), and distal colon (91.7 ± 1.5%). Within the SMP, the proximal colon had significantly lower MGL-expressing cells than the duodenum ($P < 0.05$) and the distal colon ($P < 0.01$). The use of calretinin, a Ca^{2+}-binding protein localized on both excitatory motor neurons projecting to longitudinal muscle as well as ascending interneurons, was also used for double labeling with MGL (Fig. 5). Cell counts show that MGL is expressed in the majority (>80%) of calretinin-positive cells within the MP and SMP of all the regions of the GI tract (data not shown). Inhibitory motor neurons are known to express neuronal NOS (nNOS). Using an antibody raised against nNOS, we determined that very little colocalization of MGL and NOS was observed within the MP of rat GI tract (Fig. 5).

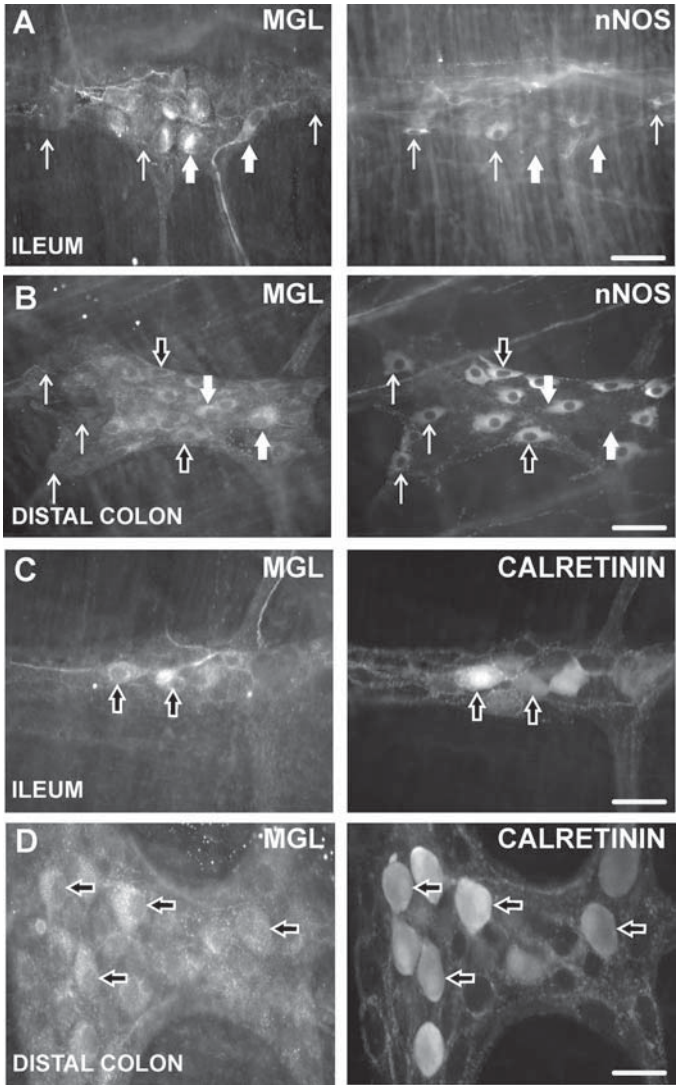

Fig. 5. Fluorescence micrographs of MGL immunoreactivity double labeled with neuronal nitric oxide synthase (nNOS) (*A* and *B*) and calretinin (*C* and *D*) in whole-mount preparations of rat myenteric plexus in the ileum (*A* and *C*) and distal colon (*B* and *D*). Single labels for MGL are in the first column, with nNOS and calretinin immunoreactivity in the second column. Enteric neurons only expressing both MGL and nNOS or calretinin are shown with open arrows. Enteric neurons expressing only nNOS are shown with thin arrows, and neurons expressing only MGL are shown with thick arrows. Scale bar: 50 μm.

MGL is functionally active in the rat ileum. The soluble fraction of extracts from rat GI tissues was assessed for the ability to hydrolyze 2-oleoylglycerol (2-OG) in vitro, according to minor modifications to the method of Vandevoorde et al. (46). By use of this assay, a gradation of activity was observed in the gut (Fig. 6*A*), such that activity in the small intestine was four to eight times higher than in the colon. Separating the mucosa in the ileum from the muscle and submucosal layers allowed determination of a much higher MGL activity in this region than in the muscle and submucosal layers, where activity was relatively low (Fig. 6*B*). MGL activity in all of the soluble fractions of GI tissue was completely inhibited in the presence of 1 μM methyl arachidonyl fluorophosphonate (MAFP, data not shown).

Additional MGL activities have been identified in mouse tissues which are associated with membrane fractions (2, 35). We, therefore, addressed whether the membrane fraction from rat GI tissue was able to hydrolyze 2-OG and whether FAAH (also present in the membrane fraction) contributes to this activity, by evaluating MGL activity in the absence and presence of the FAAH inhibitor URB597 (1 μM). In the ileal muscle and mucosal layers, membrane MGL activity was observed (Fig. 6*C*) and this was found to be insensitive to URB597 (140 ± 15 nmol·min^{-1}·mg protein^{-1} compared with 134 ± 57 in the presence of URB597). In contrast, the hydrolysis of 2-OG by membrane preparations from the ileal mucosa was reduced in the presence of URB597, indicating that FAAH contributed to this activity (521 ± 71 nmol·min^{-1}·mg protein^{-1} basal activity compared with 318 ± 27 in the presence of URB597). No regional differences of URB597-sensitivity was observed in the membrane fractions of samples of duodenum, ileum, or colon (Fig. 6*D*). The ability of URB602 (10^{-7} to 10^{-4} M) to inhibit MGL was assessed by use of preparations from the rat ileal mucosa because this tissue had the highest levels of MGL activity (Fig. 6*E*). URB602 was able to inhibit 2-OG hydrolysis in both fractions, although the soluble fractions appear to be more sensitive to the inhibitory actions of URB602. MAFP (10^{-11} to 10^{-5} M) was less potent an inhibitor of MGL activity in the membrane fraction (conducted in the presence of 1 μM URB597) compared with soluble preparations from the ileal mucosa. The EC_{50} for MAFP inhibition of 2-OG in the soluble fraction was 0.97 nM compared with 3.34 nM in the membrane fraction. In a further study to assess the selectivity of URB602 for MGL over FAAH, URB602 (100 μM) evoked a significant ($P < 0.01$, Student's *t*-test) inhibition of ileum soluble MGL activity (reduced to 56 ± 4% of control activity levels, $n = 3$). In contrast, URB602 (100 μM) evoked a much more modest inhibition of rat liver particulate FAAH activity (reduced to 86 ± 2% of control activity levels, $P < 0.05$, $n = 3$).

The MGL inhibitor URB602 inhibits whole gut transit in mice. URB602 at doses of 20 and 40 mg/kg tended to reduce upper GI transit (Fig. 7*A*) and slow colonic propulsion (Fig. 7*B*), although these did not reach statistical significance. When taken together as whole gut transit, it was apparent that

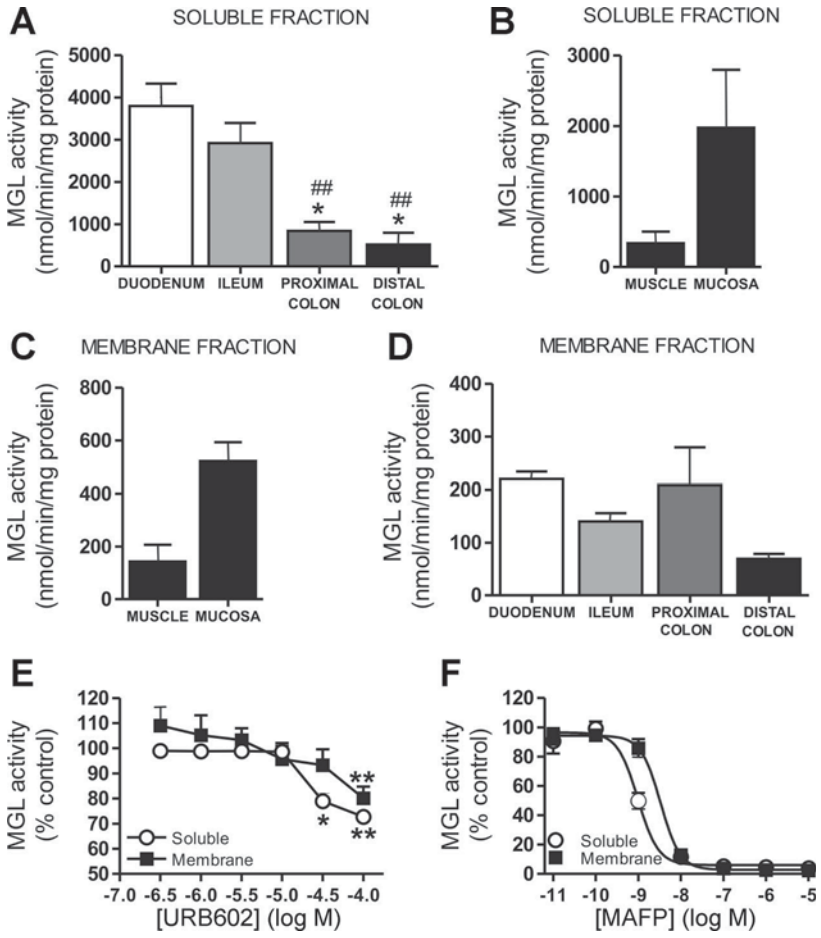

Fig. 6. MGL is active throughout the GI tract. *A*: MGL activity (2-OG hydrolysis) in the soluble fraction of full-wall-thickness samples of intestine and colon reveal that the highest activity levels are observed in the duodenum and ileum, with lower activity in the proximal and distal colon. *$P < 0.05$ vs. ileum, ##$P < 0.01$ vs. duodenum. *B* and *C*: the majority of MGL activity in the rat ileum is present in the mucosa compared with the muscle layers in both the soluble and membrane fractions. *D*: MGL activity in the membrane fraction was lower than activity observed in the soluble fraction and no regional differences were observed. *E* and *F*: comparison of the MGL activity in the rat ileal mucosa indicates that URB602 and MAFP inhibit hydrolysis more effectively in the soluble fraction. Data are means ± SE from 3 animals. *$P < 0.05$, **$P < 0.01$.

URB602 dose dependently inhibited transit ($P < 0.05$, Fig. 7*C*) compared with the vehicle control group. In CB_1 receptor-deficient mice, transit times were accelerated compared with wild-type mice, in agreement with previous reports (48). The inhibitory action of 40 mg/kg URB602 on whole gut transit was absent in these mice (Fig. 7*D*), indicating CB_1 receptor involvement in the inhibitory action. Preliminary data indicate that 40 mg/kg URB602 also attenuates upper GI transit in rats (62.6 ± 4.0% of intestine traveled compared with 75.8 ± 2.5% in vehicle-treated controls, $P < 0.05$).

DISCUSSION

We report that the endocannabinoid hydrolyzing enzyme MGL is widely distributed in the rodent GI tract. Furthermore, MGL is functionally active along the GI tract and can be inhibited by the noncompetitive MGL inhibitor URB602 (25), resulting in slowing of transit along the gut.

We show that MGL mRNA and protein are expressed within the muscle and mucosal layers of the rat ileum as well as in the duodenum, ileum, and proximal and distal colon. Semiquantification of MGL protein expression demonstrates a significantly higher amount of MGL protein in the layers of the gut that contain the enteric plexuses compared with the mucosal layer. These data fit well with the extensive expression of MGL immunoreactivity in neurons of the ENS. When examined with these approaches, there is an increasing trend of MGL protein expression from duodenum to distal colon, which potentially may account for lower levels of 2-AG reported within the colon (38).

To determine the overall regional activity levels within the GI tract, we employed an assay of 2-OG hydrolysis. MGL is a soluble, cytoplasmic enzyme associated with the cell membrane (2). Therefore, we assessed the soluble fraction from rat gastrointestinal tissues for in vitro hydrolysis of 2-OG. High levels of MGL activity were found in the ileal mucosa with relatively low levels observed within the muscle and submucosal layers, despite the apparently high levels of protein expression. In full-wall-thickness samples, MGL activity is highest in the duodenum and ileum, with lower activity observed in the colon. These data are in direct contrast to our MGL expression data, where the duodenum expressed the lowest level of protein expression. It could be the case that MGL represents only a percentage of 2-OG hydrolyzing enzymes within gastrointestinal tissues. 2-AG hydrolysis has been also reported by "novel MGL" activities present in a microglial cell line, as well as two uncharacterized enzymes, ABHD6 and ABHD12, described in the mouse brain (2). The inverse relationship between the expression levels of MGL detected by our antibody and activity in the soluble fractions of this enzyme is striking, so it might be that there is a unique regulation of 2-AG in the GI tract by a number of enzymes or that the expression of the antigenic epitope seen by the antibody does not fully reflect functional enzyme activity. Further studies are required to address this issue.

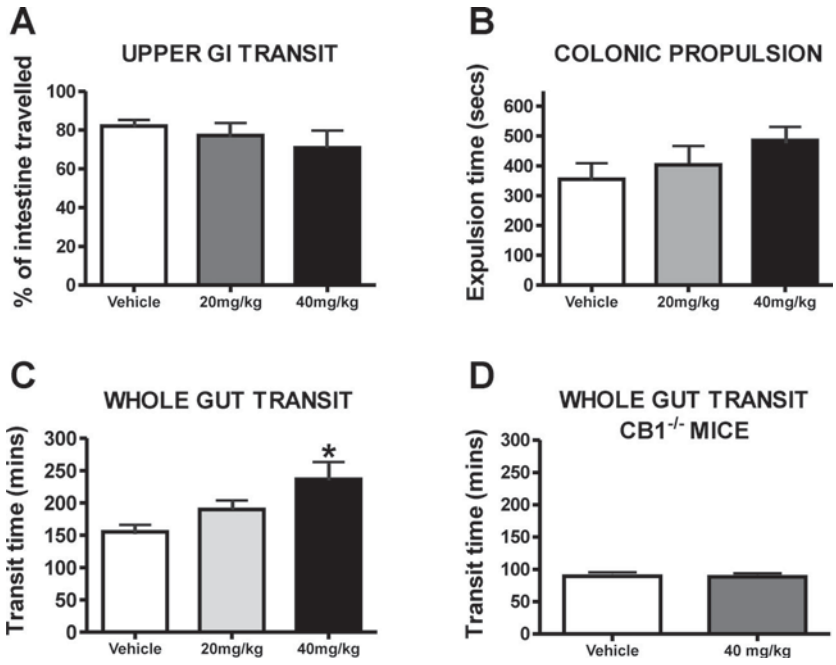

Fig. 7. Actions of the MGL inhibitor URB602 (20 and 40 mg/kg ip) on gastrointestinal motility in mice. URB602 tended to reduce upper GI transit (*A*) and increase the latency of colonic propulsion (*B*), but these effects did not reach significance. URB602 produced a dose-dependent inhibition of whole gut transit (*C*) compared with the vehicle control group (*$P < 0.05$). In CB_1 receptor-deficient mice, the inhibitory actions of 40 mg/kg URB602 on whole gut transit were absent (*D*), indicating CB_1 receptor involvement in this response. It should be noted that the whole gut transit is faster in the vehicle-treated CB_1 receptor-deficient mice than in wild-type animals.

As noted above, a novel MGL has recently been described in the mouse microglial line BV-2. These cells do not express MGL mRNA but retain the ability to hydrolyze 2-AG. Hydrolysis of 2-AG is less efficacious in BV-2 cells compared with MGL-expressing neurons and is also less sensitive to the inhibitory actions of both MAFP and URB602 (35). In neurons, MGL activity is equally distributed between membrane and soluble fractions, whereas novel MGL is enriched in the membrane fraction in BV-2 cells. To address whether novel MGL is expressed in the GI tract, we evaluated the membrane fractions of our homogenates and found low but significant levels of 2-OG hydrolyzing activity. The activity profile between mucosa and muscle was similar to that observed in the soluble fraction, but there were no regional differences in the full-thickness samples along the GI tract. In the membrane fractions, MAFP was less potent as an inhibitor of MGL activity than in the soluble fraction. To further test the differential sensitivity to MGL inhibitors, we then compared the ability of URB602 to inhibit MGL in the soluble and membrane fractions of ileal mucosa. In these experiments, the soluble fraction is more sensitive to URB602; taken together with the residual activity in the presence of MAFP we consider it likely that there is a novel MGL present in the GI tract.

The antibody we use is directed against the "classical" MGL which has been cloned and characterized. Cells expressing novel MGL do not have classical MGL mRNA but are nevertheless able to hydrolyze 2-AG. We propose that the enzyme activity we report is "total 2-AG hydrolysis" from the combined activities of classical MGL, novel MGL, and possibly ABHD6 and ABHD12 as well as potentially other, as yet unidentified, enzymes. This would also explain some of the apparent discrepancy between our expression levels, cell counts, and hydrolyzing activity, since we are only characterizing the expression profile of a proportion of the total 2-AG hydrolyzing enzymes.

There has been some controversy about the selectivity of URB602 for MGL over FAAH (46). In our hands URB602 significantly inhibited MGL activity, whereas the same concentration only slightly inhibited FAAH activity. These data are in agreement with studies in BV-2 cell lines (35) and brain slice cultures (27), in which a small inhibition of FAAH activity was observed at higher concentrations of URB602. These studies report no accompanying rise in anandamide in the preparations and so indicate that this small effect on FAAH is unlikely to be relevant.

The chemical coding of neurons within the ENS has been well established (7, 26). We report MGL to be expressed on the majority of enteric neurons, including a subpopulation of excitatory motor neurons that innervate longitudinal muscle within the gut responsible for regulation of motility patterns (7, 26). Curiously, this enzyme was virtually absent from neurons that express NOS, which are inhibitory motor neurons innervating the circular muscle, as well as a population of descending interneurons (7, 26). It is interesting to note that these neurons do not express the CB_1 or CB_2 receptor (16, 43), whereas, like MGL, most other populations express the cannabinoid receptors. The functional significance of this observation remains to be determined.

The presence of MGL within the ENS may indicate a functional role in regulating GI motility. To test the idea that inhibition of MGL could influence motility, we evaluated URB602 on upper GI transit, colonic propulsion, and whole gut transit times. We found that URB602 was able to dose dependently attenuate whole gut transit in mice. Although there was not a significant action on upper GI transit or colonic propulsion, there was a trend to slow motility in both assays that would contribute to the overall attenuation of the whole gut transit time. The actions of URB602 were absent in mice deficient for the CB_1 receptor, which would indicate the mechanism of action is by raising local 2-AG levels to activate inhibitory CB_1 receptors expressed in the ENS. The sources of 2-AG in the gut are currently unknown. Preliminary immunohistochemical studies indicate that diacylglycerol lipase beta (DGL-β), an enzyme that is important for 2-AG synthesis, is

present in the rat MP (M. Duncan and K. A. Sharkey, unpublished observations). The expression of MGL on cell bodies and nerve fibers suggests the ENS contains the machinery for degradation of 2-AG and suggests that MGL could play a role as part of the endocannabinoid system in the physiological regulation of the ENS in the GI motility.

The main focus of this paper is the role of MGL as an endocannabinoid hydrolyzing enzyme, but this enzyme does have other functions. The high expression we observe in the epithelia is in agreement with a previous study (19) using the intestinal Caco-2 cell line. This cell line can be used as a model of mature villus cells in the intestinal epithelium, and the authors report that they contain the MGL gene and are able to metabolize *sn*-2-monoacylglycerol (19). Intestinal MGL can also be regulated by diet: rats being fed a high-fat diet had significantly elevated MGL expression and activity compared with the low-fat diet group (5). These studies indicate MGL plays an important role in lipid regulation and metabolism. Nomura and coworkers (36) recently reported potent inhibition of MGL using organophosphorus (OP) compounds. In their assay, OP inhibition of MGL resulted in increased 2-AG levels and decreased arachidonic acid levels, which in the gut would have anti-inflammatory properties. Furthermore, the authors demonstrate that OP compounds activate CB_1 receptors by the metabolic stabilization of 2-AG, which would explain why the effects of MGL inhibition we observed were absent in CB_1 receptor-deficient mice. The widespread distribution of MGL throughout the gut, we report, not only contributes to knowledge of endocannabinoid signaling within the gut but suggests that MGL may be a suitable target in the treatment of obesity or as an anti-inflammatory agent.

In conclusion, we report that MGL is functionally expressed within the GI tract and novel 2-AG hydrolyzing enzymes are also present in cell membrane fractions in the gut. MGL is present in neurons and epithelia and has different activity profiles along the gut, indicating this enzyme could be involved in the regulation of many physiological processes. Despite the low potency of URB602, we were able to demonstrate inhibition of MGL in the GI tract in both in vitro and in vivo assays. These data add further to the elucidation of the endocannabinoid system and the GI tract. URB602 might also be used as a lead compound to develop more potent and specific MGL inhibitors to further elucidate the role of MGL in GI function.

ACKNOWLEDGMENTS

We thank Winnie Ho for genotyping the CB_1 gene-deficient mice used in this study and Hong Zhang for assistance with the PCR study.

GRANTS

This research was supported by the Canadian Institutes of Health Research (CIHR, to K. A. Sharkey and K. D. Patel). K. A. Sharkey is an Alberta Heritage Foundation for Medical Research (AHFMR) Medical Scientist and the Crohn's and Colitis Foundation of Canada Chair in IBD Research. M. Duncan is an AHFMR and Canadian Association of Gastroenterology/CIHR/Janssen-Ortho/Astra Zeneca Postdoctoral fellow. K. Patel is a Canada Research Chair and an AHFMR Senior Scholar. A. Patel is supported by a Doctoral Training Award from the Medical Research Council of the United Kingdom.

REFERENCES

1. **Bisogno T, Ligresti A, Di Marzo V.** The endocannabinoid signalling system: biochemical aspects. *Pharmacol Biochem Behav* 81: 224–238, 2005.
2. **Blankman JL, Simon GM, Cravatt BF.** A comprehensive profile of brain enzymes that hydrolyze the endocannabinoid 2-arachidonoylglycerol. *Chem Biol* 14: 1347–1356, 2007.
3. **Broccardo M, Improta G, Tabacco A.** Central effect of SNC 80, a selective and systemically active delta-opioid receptor agonist, on gastrointestinal propulsion in the mouse. *Eur J Pharmacol* 342: 247–251, 1998.
4. **Capasso R, Matias I, Lutz B, Borrelli F, Capasso F, Marsicano G, Mascolo N, Petrosino S, Monory K, Valenti M, Di Marzo V, Izzo AA.** Fatty acid amide hydrolase controls mouse intestinal motility in vivo. *Gastroenterology* 129: 941–951, 2005.
5. **Chon SH, Zhou YX, Dixon JL, Storch J.** Intestinal monoacylglycerol metabolism: developmental and nutritional regulation of monoacylglycerol lipase and monoacylglycerol acyltransferase. *J Biol Chem* 282: 33346–33357, 2007.
6. **Comelli F, Giagnoni G, Bettoni I, Colleoni M, Costa B.** The inhibition of monoacylglycerol lipase by URB602 showed an anti-inflammatory and anti-nociceptive effect in a murine model of acute inflammation. *Br J Pharmacol* 152: 787–794. 2007.
7. **Costa M, Brookes SJ, Steele PA, Gibbins I, Burcher E, Kandiah CJ.** Neurochemical classification of myenteric neurons in the guinea-pig ileum. *Neuroscience* 75: 949–967, 1996.
8. **Cravatt BF, Giang DK, Mayfield SP, Boger DL, Lerner RA, Gilula NB.** Molecular characterization of an enzyme that degrades neuromodulatory fatty-acid amides. *Nature* 384: 83–87, 1996.
9. **Deutsch DG, Chin SA.** Enzymatic synthesis and degradation of anandamide, a cannabinoid receptor agonist. *Biochem Pharmacol* 46: 791–796, 1993.
10. **Devane WA, Hanus L, Breuer A, Pertwee RG, Stevenson LA, Griffin G, Gibson D, Mandelbaum A, Etinger A, Mechoulam R.** Isolation and structure of a brain constituent that binds to the cannabinoid receptor. *Science* 258: 1946–1949, 1992.
11. **Di Marzo V.** Endocannabinoids: synthesis and degradation. *Rev Physiol Biochem Pharmacol* 160: 1–24, 2008.
12. **Di Marzo V, Bifulco M, De Petrocellis L.** The endocannabinoid system and its therapeutic exploitation. *Nat Rev Drug Discov* 3: 771–784, 2004.
13. **Dinh TP, Carpenter D, Leslie FM, Freund TF, Katona I, Sensi SL, Kathuria S, Piomelli D.** Brain monoglyceride lipase participating in endocannabinoid inactivation. *Proc Natl Acad Sci USA* 99: 10819–10824, 2002.
14. **Dinh TP, Freund TF, Piomelli D.** A role for monoglyceride lipase in 2-arachidonoylglycerol inactivation. *Chem Phys Lipids* 121: 149–158, 2002.
15. **Duncan M, Davison JS, Sharkey KA.** Review article: endocannabinoids and their receptors in the enteric nervous system. *Aliment Pharmacol Ther* 22: 667–683, 2005.
16. **Duncan M, Mouihate A, Mackie K, Keenan CM, Buckley NE, Davison JS, Patel KD, Pittman QJ, Sharkey KA.** Cannabinoid CB_2 receptors in the enteric nervous system modulate gastrointestinal contractility in lipopolysaccharide-treated rats. *Am J Physiol Gastrointest Liver Physiol* 295: G78–G87, 2008.
17. **Goparaju SK, Ueda N, Taniguchi K, Yamamoto S.** Enzymes of porcine brain hydrolyzing 2-arachidonoylglycerol, an endogenous ligand of cannabinoid receptors. *Biochem Pharmacol* 57: 417–423, 1999.
18. **Guindon J, Desroches J, Beaulieu P.** The antinociceptive effects of intraplantar injections of 2-arachidonoyl glycerol are mediated by cannabinoid CB_2 receptors. *Br J Pharmacol* 150: 693–701, 2007.
19. **Ho SY, Delgado L, Storch J.** Monoacylglycerol metabolism in human intestinal Caco-2 cells: evidence for metabolic compartmentation and hydrolysis. *J Biol Chem* 277: 1816–1823, 2002.
20. **Hohmann AG, Suplita RL, Bolton NM, Neely MH, Fegley D, Mangieri R, Krey JF, Walker JM, Holmes PV, Crystal JD, Duranti A, Tontini A, Mor M, Tarzia G, Piomelli D.** An endocannabinoid mechanism for stress-induced analgesia. *Nature* 435: 1108–1112, 2005.
21. **Howlett AC, Barth F, Bonner TI, Cabral G, Casellas P, Devane WA, Felder CC, Herkenham M, Mackie K, Martin BR, Mechoulam R, Pertwee RG.** International Union of Pharmacology. XXVII. Classification of cannabinoid receptors. *Pharmacol Rev* 54: 161–202, 2002.
22. **Izzo AA, Camilleri M.** Emerging role of cannabinoids in gastrointestinal and liver diseases: basic and clinical aspects. *Gut* 57: 1140–1155, 2008.
23. **Izzo AA, Fezza F, Capasso R, Bisogno T, Pinto L, Iuvone T, Esposito G, Mascolo N, Di Marzo V, Capasso F.** Cannabinoid CB1-receptor mediated regulation of gastrointestinal motility in mice in a model of intestinal inflammation. *Br J Pharmacol* 134: 563–570, 2001.

24. **Karlsson M, Reue K, Xia YR, Lusis AJ, Langin D, Tornqvist H, Holm C.** Exon-intron organization and chromosomal localization of the mouse monoglyceride lipase gene. *Gene* 272: 11–18, 2001.
25. **King AR, Duranti A, Tontini A, Rivara S, Rosengarth A, Clapper JR, Astarita G, Geaga JA, Luecke H, Mor M, Tarzia G, Piomelli D.** URB602 inhibits monoacylglycerol lipase and selectively blocks 2-arachidonoylglycerol degradation in intact brain slices. *Chem Biol* 14: 1357–1365, 2007.
26. **Lomax AE, Furness JB.** Neurochemical classification of enteric neurons in the guinea-pig distal colon. *Cell Tissue Res* 302: 59–72, 2000.
27. **Makara JK, Mor M, Fegley D, Szabo SI, Kathuria S, Astarita G, Duranti A, Tontini A, Tarzia G, Rivara S, Freund TF, Piomelli D.** Selective inhibition of 2-AG hydrolysis enhances endocannabinoid signaling in hippocampus. *Nat Neurosci* 8: 1139–1141, 2005.
28. **Marsicano G, Wotjak CT, Azad SC, Bisogno T, Rammes G, Cascio MG, Hermann H, Tang J, Hofmann C, Zieglgansberger W, Di Marzo V, Lutz B.** The endogenous cannabinoid system controls extinction of aversive memories. *Nature* 418: 530–534, 2002.
29. **Massa F, Marsicano G, Hermann H, Cannich A, Monory K, Cravatt BF, Ferri GL, Sibaev A, Storr M, Lutz B.** The endogenous cannabinoid system protects against colonic inflammation. *J Clin Invest* 113: 1202–1209, 2004.
30. **Mathison R, Ho W, Pittman QJ, Davison JS, Sharkey KA.** Effects of cannabinoid receptor-2 activation on accelerated gastrointestinal transit in lipopolysaccharide-treated rats. *Br J Pharmacol* 142: 1247–1254, 2004.
31. **Matias I, Di Marzo V.** Endocannabinoids and the control of energy balance. *Trends Endocrinol Metab* 18: 27–37, 2007.
32. **Mechoulam R, Ben-Shabat S, Hanus L, Ligumsky M, Kaminski NE, Schatz AR, Gopher A, Almog S, Martin BR, Compton DR, Pertwee RG, Griffin G, Bayewitch M, Barg J, Vogel Z.** Identification of an endogenous 2-monoglyceride, present in canine gut, that binds to cannabinoid receptors. *Biochem Pharmacol* 50: 83–90, 1995.
33. **Moore SA, Nomikos GG, Dickason-Chesterfield AK, Schober DA, Schaus JM, Ying BP, Xu YC, Phebus L, Simmons RM, Li D, Iyengar S, Felder CC.** Identification of a high-affinity binding site involved in the transport of endocannabinoids. *Proc Natl Acad Sci USA* 102: 17852–17857, 2005.
34. **Mouihate A, Clerget-Froidevaux MS, Nakamura K, Negishi M, Wallace JL, Pittman QJ.** Suppression of fever at near term is associated with reduced COX-2 protein expression in rat hypothalamus. *Am J Physiol Regul Integr Comp Physiol* 283: R800–R805, 2002.
35. **Muccioli GG, Xu C, Odah E, Cudaback E, Cisneros JA, Lambert DM, Lopez Rodriguez ML, Bajjalieh S, Stella N.** Identification of a novel endocannabinoid-hydrolyzing enzyme expressed by microglial cells. *J Neurosci* 27: 2883–2889, 2007.
36. **Nomura DK, Hudak CS, Ward AM, Burston JJ, Issa RS, Fisher KJ, Abood ME, Wiley JL, Lichtman AH, Casida JE.** Monoacylglycerol lipase regulates 2-arachidonoylglycerol action and arachidonic acid levels. *Bioorg Med Chem Lett*. In press.
37. **Pacher P, Gao B.** Endocannabinoids and liver disease. III. Endocannabinoid effects on immune cells: implications for inflammatory liver diseases. *Am J Physiol Gastrointest Liver Physiol* 294: G850–G854, 2008.
38. **Pinto L, Izzo AA, Cascio MG, Bisogno T, Hospodar-Scott K, Brown DR, Mascolo N, Di Marzo V, Capasso F.** Endocannabinoids as physiological regulators of colonic propulsion in mice. *Gastroenterology* 123: 227–234, 2002.
39. **Pol O, Ferrer I, Puig MM.** Diarrhea associated with intestinal inflammation increases the potency of mu and delta opioids on the inhibition of gastrointestinal transit in mice. *J Pharmacol Exp Ther* 270: 386–391, 1994.
40. **Pol O, Sanchez B, Puig MM.** Peripheral effects of opioids in a model of intestinal inflammation in mice. *Pharmacology* 53: 340–350, 1996.
41. **Sharkey KA, Coggins PJ, Tetzlaff W, Zwiers H, Bisby MA, Davison JS.** Distribution of growth-associated protein, B-50 (GAP-43) in the mammalian enteric nervous system. *Neuroscience* 38: 13–20, 1990.
42. **Stella N, Schweitzer P, Piomelli D.** A second endogenous cannabinoid that modulates long-term potentiation. *Nature* 388: 773–778, 1997.
43. **Storr M, Sibaev A, Marsicano G, Lutz B, Schusdziarra V, Timmermans JP, Allescher HD.** Cannabinoid receptor type 1 modulates excitatory and inhibitory neurotransmission in mouse colon. *Am J Physiol Gastrointest Liver Physiol* 286: G110–G117, 2004.
44. **Storr MA, Sharkey KA.** The endocannabinoid system and gut-brain signalling. *Curr Opin Pharmacol* 7: 575–582, 2007.
45. **Storr MA, Yuce B, Andrews CN, Sharkey KA.** The role of the endocannabinoid system in the pathophysiology and treatment of irritable bowel syndrome. *Neurogastroenterol Motil* 20: 857–868, 2008.
46. **Vandevoorde S, Jonsson KO, Labar G, Persson E, Lambert DM, Fowler CJ.** Lack of selectivity of URB602 for 2-oleoylglycerol compared to anandamide hydrolysis in vitro. *Br J Pharmacol* 150: 186–191, 2007.
47. **Wright KL, Duncan M, Sharkey KA.** Cannabinoid CB_2 receptors in the gastrointestinal tract: a regulatory system in states of inflammation. *Br J Pharmacol* 153: 263–270, 2008.
48. **Yuece B, Sibaev A, Broedl UC, Marsicano G, Goke B, Lutz B, Allescher HD, Storr M.** Cannabinoid type 1 receptor modulates intestinal propulsion by an attenuation of intestinal motor responses within the myenteric part of the peristaltic reflex. *Neurogastroenterol Motil* 19: 744–753, 2007.